HYGROTHERMALLY STABLE LAMINATED COMPOSITES FOR OPTIMAL EXTENSION TWIST COUPLING IN CLOSED CELL CONFIGURATION

by

SEAN MUDER

Presented to the Faculty of the Graduate School of
The University of Texas at Arlington in Partial Fulfillment
of the Requirements
for the Degree of

MASTER OF SCIENCE IN AEROSPACE ENGINEERING

THE UNIVERSITY OF TEXAS AT ARLINGTON

May 2012

Copyright © by Sean Christopher Muder 2012

All Rights Reserved

ACKNOWLEDGEMENTS

I wish to thank my advisor, Dr. Erian Armanios, who has provided continuous support and encouragement. I am grateful for his motivational advice and for the freedom he has given me in my research pursuits. His support has extended well beyond my educational success into my well-being and personal interests. I could not ask for a more influential and compassionate advisor.

I wish to thank my co-advisor, Dr. Robert Haynes, who has played a key role in my success. His willingness and availability to provide guidance and advice have circumvented many potential problems and have helped me develop my engineering skills. I also want to thank my committee members Dr. Wen Chan and Dr. Kent Lawrence for their time and attention. Dr. Chan's advice and demanding courses have helped me build a solid foundation of knowledge in my area of interest. He has also taken an interest in my success and has been consistently available to provide support and advice. I wish to thank my office-mate Dr. Xinyuan Tan for her generosity, support, and encouragement.

Sincerely, I would like to thank my family and friends for their unconditional love and support. Specifically, I wish to thank Leah Cox for her support and most importantly for helping me maintain a positive attitude during a particularly tough last year. I would like to thank my brother, Chase Muder, who has been my best friend since the day we met and has always been there for me. I would like to express my sincere gratitude to my mother and father, Christopher and Laurie Muder, who continually had confidence in my abilities even when others may have not. Their love, support, patience, and guidance have fueled the desire to pursue my goals. Without them, I certainly would not be the person I am today.

April 20, 2012

ABSTRACT

HYGROTHERMALLY STABLE LAMINATED COMPOSITES

FOR OPTIMAL EXTENSION TWIST COUPLING

IN CLOSED CELL CONFIUGURATION

Sean Christopher Muder, M.S.

The University of Texas at Arlington, 2012

Supervising Professor: Erian Armanios

An optimization routine utilizing the sequential quadratic programming method is used to develop laminates that are hygrothermally stable in flat-strip configuration and are optimal for extension twist coupling in closed cell configuration. The performance of the laminates obtained from the optimization in terms of the level of extension twist coupling and hygrothermal stability are evaluated and compared to laminates from a previous routine. A parametric study is conducted to illustrate the relationships between the geometric dimensions of a representative closed cell section and the level of extension twist coupling. Results from the parametric study suggested a more practical optimization approach in which the trend between extension twist compliance and stiffness is the optimization goal. This approach produces laminates that are more material efficient and have a better trend between extension twist coupling and stiffness. A case study on a blade section of an XV-15 tilt rotor illustrates the advantage of the new optimization approach.

TABLE OF CONTENTS

LIST OF ILLUSTRATIONS

LIST OF TABLES

CHAPTER 1

INTRODUCTION & LITERATURE SURVEY

1.1 Introduction

Composite laminates have the potential for coupling between in-plane and out-of-plane deformations modes. This provides designers with the capability to implement passive static and dynamic responses into their structures[1]. The pioneering work of Krone[2] demonstrated that varying degrees of curvature can be obtained in structures that are subject to variations in mechanical and thermal induced stress. Applications ranging from the sports equipment to space structures stand to benefit from this capability. Recent developments have reduced aeroelastic divergent twisting in forward swept wing aircraft by implementing bend-twist coupling into the structure of the wing[3]. Other work[4] suggests that the variation of the twist rate of the blade on tilt-rotor aircraft through the application of extension twist coupling has the potential to improve performance.

The possibility for improvement in performance of many applications has provided motivation to develop laminates and structures that exhibit the desired coupling behavior. Past research[5,6] has demonstrated that high levels of coupling can be achieved in laminates and structures by arranging the stacking sequence and fiber orientation in a specific manner. Recent improvements in manufacturing processes such as automated fiber lay-up machines and co-curing methods have made more specific layup angles a reality. This suggests that more consideration should be given to the ply orientations of composite applications.

This study is focused on developing hygrothermally stable laminates that are optimal for tension torsion response in closed cell configuration. The performance of the laminates in closed cell configuration is evaluated in terms of the level of extension twist compliance and hygrothermal stability.

1.2 Literature Survey

1.2.1 Classical Lamination Theory

In order to gain an understanding and appreciation of extension twist coupling a review of Classical Lamination Theory (CLT)[1] is required. According to CLT, the constitutive relationships for a flat composite strip are expressed as

$$\begin{bmatrix} N_{xx} \\ N_{yy} \\ N_{xy} \\ M_{xx} \\ M_{yy} \\ M_{xy} \end{bmatrix} = \begin{bmatrix} A_{11} & A_{12} & A_{13} & B_{11} & B_{12} & B_{13} \\ A_{12} & A_{22} & A_{26} & B_{12} & B_{22} & B_{26} \\ A_{16} & A_{26} & A_{66} & B_{16} & B_{26} & B_{66} \\ B_{11} & B_{12} & B_{13} & D_{11} & D_{12} & D_{16} \\ B_{12} & B_{22} & B_{26} & D_{12} & D_{22} & D_{26} \\ B_{16} & B_{26} & B_{66} & D_{16} & D_{26} & D_{66} \end{bmatrix} \begin{bmatrix} \varepsilon_{xx} \\ \varepsilon_{yy} \\ \gamma_{xy} \\ \kappa_{xx} \\ \kappa_{yy} \\ \kappa_{xy} \end{bmatrix} - \begin{bmatrix} N_{xx} \\ N_{yy} \\ N_{xy} \\ M_{xx} \\ M_{yy} \\ M_{xy} \end{bmatrix}^{(T,H)} \qquad [1.1]$$

where N_{xx}, N_{yy}, N_{xy}, M_{xx}, M_{yy}, and M_{xy} are the mechanical stress resultants, ε_{xx}, ε_{yy}, γ_{xy}, κ_{xx}, κ_{yy}, and κ_{xy}, are the mid-plane strains and curvatures. The in-plane, A_{ij}, coupling, B_{ij}, and bending, D_{ij}, stiffness coefficients are defined as

$$\begin{aligned} A_{ij} &= \sum_{k=1}^{n} \overline{Q}_{ij(k)} \left(h_k - h_{k-1}\right) \\ B_{ij} &= \frac{1}{2} \sum_{k=1}^{n} \overline{Q}_{ij(k)} \left(h_k^2 - h_{k-1}^2\right) \\ D_{ij} &= \frac{1}{3} \sum_{k=1}^{n} \overline{Q}_{ij(k)} \left(h_k^3 - h_{k-1}^3\right) \end{aligned} \qquad [1.2]$$

$\left[\overline{Q}\right]_k$ and h_k represent the transformed reduced stiffness and the distance relative to the mid-plane of the laminate for the k^{th} ply. The hygrothermal stress resultants are given as

$$\begin{aligned} \begin{bmatrix} N_{xx} \\ N_{yy} \\ N_{xy} \end{bmatrix}^{(T,H)} &= \left(\Delta T, \Delta H\right) \sum_{k=1}^{n} \left[\overline{Q}\right]_k \left\{\overline{\alpha}, \overline{\beta}\right\}_k \left(h_k - h_{k-1}\right) \\ \begin{bmatrix} M_{xx} \\ M_{yy} \\ M_{xy} \end{bmatrix}^{(T,H)} &= \frac{1}{2} \left(\Delta T, \Delta H\right) \sum_{k=1}^{n} \left[\overline{Q}\right]_k \left\{\overline{\alpha}, \overline{\beta}\right\}_k \left(h_k^2 - h_{k-1}^2\right) \end{aligned} \qquad [1.3]$$

where $\{\bar{\alpha}, \bar{\beta}\}_k$ are the transformed in-plane thermal and moisture expansion coefficients for the k^{th} ply. ΔT and ΔH denote the thermal and hygral change, respectively.

Inverting the relationships in Eq. 1.4 and eliminating the hygrothermal stress resultants, the equation that relates the strains to compliance components and mechanical stress resultants becomes

$$\begin{bmatrix} \varepsilon_{xx} \\ \varepsilon_{yy} \\ \gamma_{xy} \\ \kappa_{xx} \\ \kappa_{yy} \\ \kappa_{xy} \end{bmatrix} = \begin{bmatrix} \alpha_{11} & \alpha_{12} & \alpha_{13} & \beta_{11} & \beta_{12} & \beta_{16} \\ \alpha_{12} & \alpha_{22} & \alpha_{26} & \beta_{21} & \beta_{22} & \beta_{26} \\ \alpha_{16} & \alpha_{26} & \alpha_{66} & \beta_{61} & \beta_{62} & \beta_{66} \\ \beta_{11} & \beta_{21} & \beta_{61} & \delta_{11} & \delta_{12} & \delta_{16} \\ \beta_{12} & \beta_{22} & \beta_{62} & \delta_{12} & \delta_{22} & \delta_{26} \\ \beta_{16} & \beta_{26} & \beta_{66} & \delta_{16} & \delta_{26} & \delta_{66} \end{bmatrix} \begin{bmatrix} N_{xx} \\ N_{yy} \\ N_{xy} \\ M_{xx} \\ M_{yy} \\ M_{xy} \end{bmatrix} \qquad [1.4]$$

From this relationship the couplings between deformations modes depend on the values of the off-diagonal compliance coefficients α_{ij}, β_{ij} and δ_{ij}, which are dependent on the material, fiber orientation, and stacking sequence. Assuming a fully populated compliance matrix, an introduction of an axial stress resultant N_{xx} will induce normal, shear, and curvature deformation. This is the unique property of composites materials that yields designers new capabilities.

1.2.2 Extension Twist Coupling- Flat Laminate Strip

In a composite laminate, extension twist coupling occurs as a result of in-plane extension shear coupling associated with plies that are layed-up off axis. Laminates containing plies that shear in opposite directions with respect to the mid-plane of the laminate strip produce an out-of-plane twisting deformation[7] as shown in Figure 1.1.

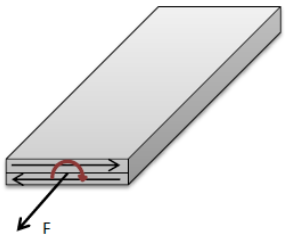

Figure 1.1 Mechanism for extension twist coupling in flat strip configuration

The most basic type of laminate that incorporates extension twist coupling is the angle ply laminate $[\pm\theta]$. These types of laminates produce high levels of extension twist coupling, but are susceptible to hygrothermal instability. This type of instability is characterized by out of plane warping caused by temperature or moisture changes. For many applications such as rotor blade and wind turbines these instabilities are typically undesirable and should be eliminated for proper functionality.

Hygrothermal stability ensures that there are no mid-plane curvatures induced by a temperature change. Conventionally in composite applications this is ensured by using symmetric stacking sequences. These types of sequences preclude the possibility of extension twist coupling since the resulting coupling stiffness matrix, [B] in Eq. 1.1, is identically zero.

In order to eliminate the hygrothermal instabilities while maintaining the extension twist coupling behavior, Winckler[8] introduced a laminate of the form $[\theta/(\theta-90)_2/\theta/-\theta/(\theta-90)_2/-\theta]$. This laminate ensures hygrothermal stability and allows for extension twist coupling by nesting a hygrothermally isotropic sublaminate of the form $[0/90]_s$ into an anti-symmetric angle ply laminate $[\pm\theta]$. Although this laminate does not produce nearly as high tension torsion coupling as the angle ply laminate, it is not subject to thermally induced warping. Recently, a new method for obtaining optimal hygrothermally stable stacking sequences was developed by Haynes *et a.l*[5] which yielded sequences that performed over 80% better than the Winckler type sequence. The method utilizes the sequential quadratic programming implementation (SQP) in MATLAB. The routine begins with a random initialized stacking sequence which meets the necessary and sufficient conditions derived by Haynes *et al.*[5] for hygrothermal stability. Two separate conditions for hygrothermal stability are derived in the work. The first, denoted as Condition A, is satisfied by ensuring that the normal non-mechanical stress resultants are equal, and that the non-mechanical shear and moment resultants are zero. The second condition, denoted as Condition B, is satisfied by ensuring that the coupling stiffness matrix is zero.

The objective function of the routine is related to the twist rate caused by an applied axial force. The twist rate is derived from the constitutive relationship noted in Eq. 1.4 that relates the applied stress resultants to the mid-plane strains and curvatures. It is given by the following

$$\varphi = \frac{1}{2}\left(nt\beta_{16}\sigma_0 + \kappa_{xy}^{(T,H)}\right) \qquad [1.6]$$

where n and t are the number of plies and thickness, respectively, β_{16} is the compliance coefficient that relates the axial stress resultant to the midplane curvature κ_{xy}, σ_o is the applied stress, and $\kappa_{xy}^{(T,H)}$ is the hygrothermally induced curvature. Since the input constraint ensures hygrothermal stability, the hygrothermally induced curvature is zero and the objective function chosen to be maximized by the optimizer is

$$F = \beta_{16}^2 \qquad [1.7]$$

A similar approach is used throughout this study to find optimal extension twist, optimal extension shear laminates, and optimal laminates for box beam configuration.

1.2.3 Closed Cell Configuration

The improvement in the level of extension twist coupling realized by the optimized laminates in the previous work provides potential for improvement in a number of applications. However, direct application of the laminates is not ideal for most purposes, and it is usually necessary that the laminates be introduced into structural configurations.

The single closed cell configuration is one of the most basic configurations that has a wide range of applications. The high level of torsional and bending stiffness makes them ideal to serve as load carrying members. Similarly to the manner in which extension twist coupling is integrated into flat strips, can box beams be designed to exhibit coupling. This can be done by wrapping a laminate exhibiting extension shear coupling around a mandrel to form a

circumferentially uniform stiffness configuration. When an axial force is applied, the laminates in the sides of the box beam shear in opposite directions with respect to the mid plane. This produces a continuous shear flow that generates an out of plane twist deformation[9].

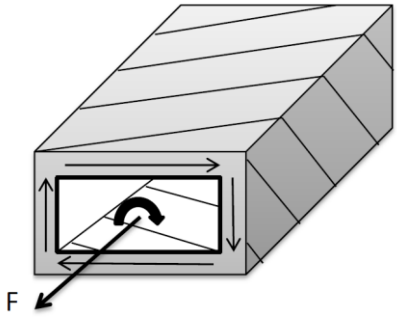

Figure 1.2 Mechanism for extension twist coupling in closed cell configuration

1.2.3.1 Closed Cell Beam Theories

The incorporation of the coupled deformation modes of composite beams into theory has been extensively pursued in the past. Lentz[9] provides a brief overview of the previous work. He noted that the majority of the approaches assume a displacement field and as a result there is significant variation between the resulting deformation estimated by the theories for various loading conditions. The most accurate and computational efficient approach suggested was developed by Berdechevsky *et al.*[10] This approach does not assume a displacement field, but instead the displacements are derived using an asymptotic approach. The key elements of the theory are outlined in the following section for convenience.

1.2.3.2 Constitutive Equation for CUS Closed Cell Sections

The variational asymptotic method was utilized to develop an equation for strain energy density for slender closed-cell sections in terms of four kinematic parameters $\lambda 1$, $\kappa 1$, $\kappa 2$, and $\kappa 3$ as

$$\Phi = \frac{1}{2}\left[C_{11}(\lambda_1)^2 + C_{22}(\kappa_1)^2 + C_{33}(\kappa_2)^2 + C_{44}(\kappa_3)^2\right] + C_{12}\lambda_1\kappa_1 + C_{13}\lambda_1\kappa_2 + C_{14}\lambda_1\kappa_1 + C_{23}k_1k_2 + C_{24}\kappa_1\kappa_3 + C_{34}\kappa_3\kappa_2 \quad [1.8]$$

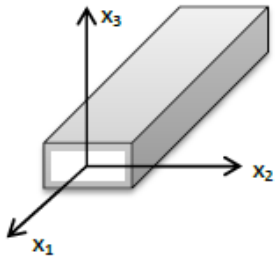

Figure 1.3 Cartesian coordinate system

where λ_1, κ_1, κ_2, and κ_3 represent the axial strain along the 1 axis and curvatures about the 1, 2, and 3 axes, respectively. Differentiation in terms of the kinematic parameters formulates the constitutive relationships, Eq. 1.9, which relates the axial force, twisting moment and bending moments to the four kinematic variables. The approximation neglects the transverse shear deformation and is valid when the ratio of the wavelength of the deformation to the characteristic diameter of the cross section remains large[11]. Thin closed-cell slender beams inherently maintain this ratio. The closed cell sections analyzed in this study maintain the thin and slender definition. The resulting stiffness matrix is given as

$$\begin{Bmatrix} F_1 \\ M_1 \\ M_2 \\ M_3 \end{Bmatrix} = \begin{bmatrix} C_{11} & C_{12} & C_{13} & C_{14} \\ C_{12} & C_{22} & C_{23} & C_{24} \\ C_{13} & C_{23} & C_{33} & C_{34} \\ C_{14} & C_{24} & C_{34} & C_{44} \end{bmatrix} \begin{Bmatrix} \lambda_1 \\ \kappa_1 \\ \kappa_2 \\ \kappa_3 \end{Bmatrix} \qquad [1.9]$$

and by inverting Eq. 1.9, the compliance coefficients can be obtained as

$$\begin{Bmatrix} \lambda_1 \\ \kappa_1 \\ \kappa_2 \\ \kappa_3 \end{Bmatrix} = \begin{bmatrix} S_{11} & S_{12} & S_{13} & S_{14} \\ S_{12} & S_{22} & S_{23} & S_{24} \\ S_{13} & S_{23} & S_{33} & S_{34} \\ S_{14} & S_{24} & S_{34} & S_{44} \end{bmatrix} \begin{Bmatrix} F_1 \\ M_1 \\ M_2 \\ M_3 \end{Bmatrix} \qquad [1.10]$$

For a circumferentially uniform stiffness configuration five of the coefficients remain nonzero and are

$$
\begin{aligned}
C_{11} &= Al & A &= A_{11} - \frac{A_{12}^2}{A_{22}} \\
C_{12} &= B \times A_e & B &= 2\left(A_{16} - \frac{A_{12}A_{26}}{A_{22}} \right) \\
C_{22} &= \frac{C}{l} A_e & C &= 4\left(A_{66} - \frac{A_{26}^2}{A_{22}} \right) \\
C_{33} &= A\oint z^2 ds - \frac{B^2}{C}\oint z^2 ds & & \\
C_{44} &= A\oint y^2 ds - \frac{B^2}{C}\oint y^2 ds & &
\end{aligned}
\qquad [1.11]
$$

where A_e and l denote the enclosed area and perimeter of the section, respectively.

1.2.4 Extension Twist Coupling Application

Work conducted by Nixon[4] recognized a potential application for extension twist coupling to be passive rotor blade control. He suggested that the incorporation of passive blade control in tilt rotor aircraft has the potential for making improvements in the power efficiency of the rotorcraft.

Tilt rotor aircraft have two different flight regimes in which the rotor speed varies. For optimal efficiency, the twist distribution of the blade should correspond to the speed of the blade. Therefore, for optimal efficiency it would be advantageous to have a blade that could alter its twist distribution with changes in rotor speed. The variations in mechanical stresses induced by the inertial forces, namely the axial stress produced by the high centrifugal force exerted on the blade, can be utilized to alter the twist distribution of the blade.

Since Nixon's introduction of this concept a large amount of literature has been dedicated to extension twist coupling and its application for passive blade control. Work conducted by Chandra and Chopra[12] demonstrated the feasibility of incorporating extension twist coupling in the blade by investigating the structural couplings in closed cell as well as open cell sections. Armanios *et al.*[13] developed a non-linear analytical model to quantify the tension torsion response in flat strip laminates. Other efforts by Armanios *et al.*[14] have designed testing methods for composite laminates with the extension twist coupling deformation mode. Work by

Lentz[9] performed an optimization which maximized the tension torsion coupling effect while minimizing hygrothermally induced curvature in a composite box beam. More recent research provided by Ozbay[15] introduced a novel concept to increase the centrifugal force on the blade using a sliding mass. This idea showed promising results for passive blade control and overcame the de-stabilization effect of additional tip mass noted by Nixon[4]. Most recently, Cross[16] and Haynes[5] developed an optimization routine with constraints on hygrothermal stability that produced laminates that are hygrothermally stable and have levels of coupling 80% higher than the Winckler-type sequences.

CHAPTER 2

MOTIVATION & RESEARCH OUTLINE

2.1 Motivation

The typical rotor blade structure is comprised of one (the blade itself) or more thin closed cell sections. Weight consideration as well as aerodynamic and inertial loads on the blade make them ideal for the application. In order to implement a passive response in the blade, it is important to understand the effect of variations in the geometry on the stiffness of the blade. In a composite rotor blade the possible variations include the size and thickness of the blade and internal blade structure, and the stacking sequence of the blade.

The increased performance realized by the optimized hygrothermally stable laminates in the previous work has motivated further investigation of the performance of optimized laminates using this routine when introduced into closed cell circumferential uniform stiffness (CUS) configuration. Work conducted by Lentz *et al.*[9] provided an optimization routine that maximized extension twist coupling while minimizing the hygrothermal warping effects. The stacking sequences generated by the routine exhibited high levels of coupling. Theoretical calculations of the hygrothermal stability using a modification of Berdechevsky's[10] theory of closed cell sections to include thermal effects[17] suggested that the sequences also exhibited minimal hygrothermal instability. A good correlation between the level of extension twist coupling predicted by the analytical model and the experimental results was demonstrated. However, an inconsistency between the theoretical hygrothermal stability predictions and experimental results existed. This has warranted a further investigation of the hygrothermal stability of these sequences.

2.2 Research Outline

The approach of this research was designed to be multi-faceted. The primary goal of the research was to develop laminates for introduction into closed cell sections that are hygrothermally stable and produce an optimal tension torsion response in closed cell configuration. In accompaniment to this, the work strives to develop a better understanding of the relationships between the area, thickness, stacking sequence, and resulting stiffness of a closed cell section.

The optimization routine used by Haynes *et al.*[5] to develop optimal sequences for coupled deformation modes in flat strip configuration is used to develop laminates that are optimal for extension twist coupling in closed cell configuration. Based on the knowledge and information obtained from the literature survey, variations of the routine are performed to develop laminates that are optimal.

The performance of the sequences obtained from the optimization routines are compared in a parametric study in which the thickness and area of a standard box beam are varied. The level of extension twist coupling and the hygrothermal stability exhibited by the sequences in box beam configuration is evaluated over the range of thicknesses and areas. Further investigation takes into account the trends between the extension twist compliance and stiffness levels. Results from this investigation suggested a more practical engineering approach in which improvement in the trend between extension twist compliance and stiffness is the goal.

Finally, a case study in which the effectiveness and feasibility of using the approach for passive blade control is conducted. Stiffness constraints from baseline requirements from the XV-15 tilt-rotor are defined and an appropriate airfoil section is chosen. The sequences from the optimization routine are introduced into the airfoil section and the thickness is increased until

the stiffness requirements are satisfied. The amount of induced blade twist caused by the variation in mechanical stress between the flight regimes is evaluated.

CHAPTER 3

OPTIMAL SEQUENCES IN CLOSED CELL SECTIONS

The optimal level of extension twist coupling attainable in single cell closed sections with constraints on hygrothermal stability is investigated in this chapter. An optimization routine utilizing the sequential quadratic programming (SQP) method outlined in Chapter 2 is altered in four different approaches to develop optimal laminates for the closed cell section. The results from the current routine are compared to a previous optimization routine designed by Lentz[9] by quantifying the level of extension twist coupling and thermally induced twist deformation.

The level of extension twist coupling in the box beam is quantified throughout this study by the S_{12} compliance coefficient from the closed form solution noted in Eq. 1.11, as it relates the axial deformation in the beam to the twisting curvature about the axial direction. Verification of these results are obtained from a finite element solution produced by the Variational Asymptotic Beam Section Analysis (VABS)[18] code.

3.1 Optimal Laminates for Extension Twist and Extension Shear

The optimization routine is used to develop optimal laminates for extension twist coupling and extension shear coupling. These laminates are introduced into box beam configuration and their performance is analyzed. The properties from the material system T300-976 Graphite/Cyanate are used for all the optimizations performed in this study and are provided in Table 3.1.

Table 3.1 Material Properties of T300-976 Graphite/Cyanate

Moduli of Elasticity	**Shear Moduli**	**Poisson's Ratio**	**Ply Thickness**
E_{11} = 135.6 GPa	$G_{12} = G_{13}$ = 4.2 GPa	$\upsilon_{12} = \upsilon_{13} = \upsilon_{23}$ =.3	tp = .0762 mm
$E_{22} = E_3$ = 9.96 GPa	G_{23} = 3.4 GPa		

3.1.1 Optimal Extension Twist Laminates

The laminates developed by Haynes for optimal extension twist in flat strip configuration with the constraint of hygrothermal stability, listed in Table 3.2, were introduced into the box beam in a CUS configuration with the dimensions shown in Figure 3.1. The sequence denoted by 8 W in Table 3.2 is a Winckler-type sequence. It is important to note that the optimality of the stacking sequences is material dependent and thus the following sequences are not optimal for all material systems.

Table 3.2 Optimal Extension Twist Laminates

Ply Count	Stacking Sequence
5	[-58.7/11.4/45/78.6/-31.3]
6	[21.2/-63.8/-48.7/48.7/63.8/-21.2]
7	[14.1/-76.9/-73.9/45/-16.1/-13.2/75.7]
8	[-21.5/72.1/57.9/-29.6/29.6/-57.9/-72.1/21.5]
9	[25.5/-79/32.5/-62.9/49.9/27.4/57/-10.6/64.9]
10	[16.2/-69.0/-65.3/31.8/42.1/-42.1/-31.8/65.3/69.0/-16.2]
8 W	$[22.5/-67.5_2/22.5/-22.5/67.5_2/-22.5]$

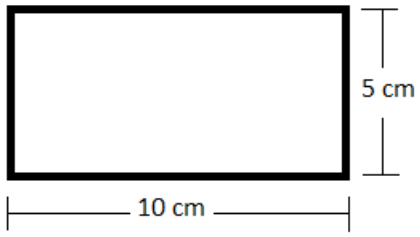

Figure 3.1 Box beam dimensions

3.1.1.1 Performance Results

The performance of the laminates in box beam configuration predicted by the closed form solution [Eqs.1.9 – 1.11] is shown in Figure 3.2. For the exception of the 9 ply sequence, it is clear that the optimal extension twist sequences do not perform well in the box beam configuration. This can be attributed directly to fact that the all of the laminates with the exception of the 9 ply laminate lack the extension shear coupling deformation mode which is the dominant factor in the closed form solution for the compliance coefficient S_{12}.

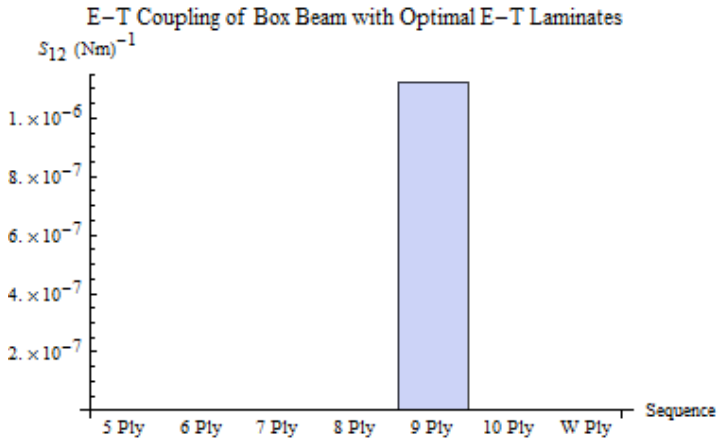

Figure 3.2 S_{12} for optimal extension twist laminates

3.1.2 Optimal Extension Shear Laminates

Recognizing the dominance of the extension shear term in the closed form solution for S_{12}, the optimization routine discussed in section 2.2 is used to develop optimal laminates for extension shear that are constrained to hygrothermal stability in flat strip configuration. These laminates are introduced into the box beam configuration and the level of coupling achievable is analyzed. Past research conducted by Lentz[9] developed optimal laminates for extension twist coupling in box beam configuration. The optimization used was a gradient based optimization that maximized the twisting curvature κ_1 while minimizing the resulting hygrothermal twist. The level of coupling and hygrothermal stability of the current and former approaches are investigated.

The stacking sequences obtained from each of the optimization routines are listed in Table 3.3. The sequences are introduced into a box beam configuration with geometric dimensions illustrated in Figure 3.3. The composite material properties are consistent with the T-300/954-3 Graphite/Cyanate material system that is used previously and for all of the optimizations in this study.

Table 3.3 Optimal Sequences for Extension Shear and Lentz *et al.* Optimal Sequences

Number of Plies	**Current**	**Lentz *et al.***
4	[22.5/ -67.5/ -67.5/ 22.5]	$[-81.84_2/\ 30.48_2]$
5	[29.9/ -74.6/ -22.5/ -74.7/ 29.8]	$[-79.04_2/28.73_3]$
6	[88.7/ -9.6/ -15.7/ 60.3/ 54.36/ -44.1]	$[-81.84_3/\ 30.48_3]$
7	[37.6/ -17.8/ -74.1/ -71.4/ 33.9/ -62.2/20.1]	$[-79.86_3/\ 29.33_4]$
8	[27.7/-60.3/30.3/-61.2/ -62.5/ 27.6/-65.0/25.4]	$[-78.33_4/\ 28.13_4]$

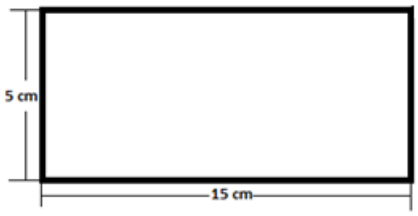

Figure 3.3 Box beam dimensions

3.1.2.1 Performance Results

The performance of the laminates predicted by the closed form solution is shown in Figure 3.4 and a finite element code called VABS is used for verification. The VABS code simplifies the nonlinear three-dimensional analysis of slender structures into a two dimensional cross sectional analysis and a one dimensional beam analysis. Using a finite element mesh of the desired cross section containing the material and geometric properties of the section, the code generates an approximation in the form of two 4x4 stiffness matrix that describe the structural properties of the beam[17].

The results illustrated in Figure 3.4 indicate that the Lentz[9] optimization results, denoted by an L in the figure, yield a level of coupling that is approximately 28% and 42% higher for the four and eight ply laminates compared respectively, and significantly better for the five, six and seven ply laminates. The average difference between the closed form solution and VABS solution is less than 1%.

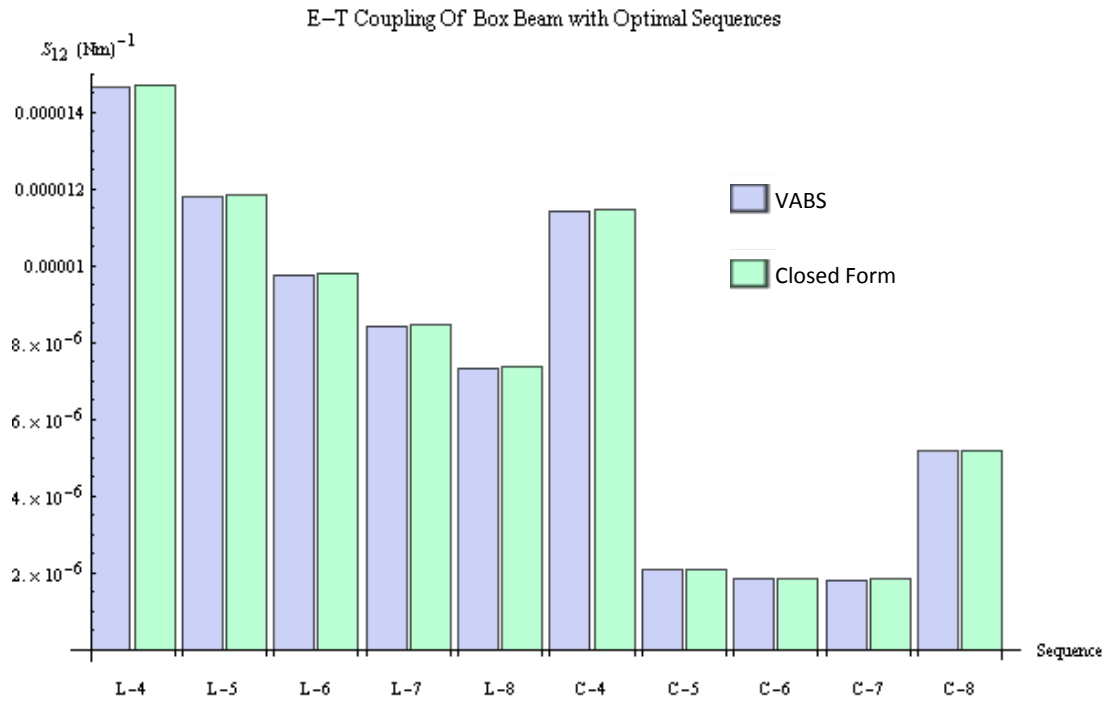

Figure 3.4 Level of coupling in a box beam with the current and former optimal laminates

3.2 Closed Cell Section Optimal Laminates

The optimization routine is taken a step further by changing the objective function from the previous optimizations for extension twist and extension shear. After recognizing the significant contribution of the α_{16} term in the closed for solution, the laminates were optimized for extension shear. It is undeniable, however, that there are other compliance coefficient terms in the closed form solution that may have an effect on the level of coupling. To evaluate the extent that the less significant compliance coefficients present in the closed form solution for S_{12} have an effect on the coupling, the objective function is changed to

$$F = \frac{B}{B^2 - AC} \qquad [3.1]$$

where coefficients A, B and C are defined in Eq.1.11. Similarly to the optimizations for the extension twist and extension shear laminates, this optimization maintains the constraint on

hygrothermal stability in flat strip configuration. However, it should be noted that this does not guarantee hygrothermal stability in box beam configuration. This is discussed in further depth in section 3.4.

The results from the optimization are listed in Table 3.4. The performance of the laminates is shown in Figure 3.5. The laminates obtained from the optimization with the E-T compliance coefficient, S_{12}, as the objective function are denoted by S followed by the corresponding ply count, and the laminates obtained from the optimization with extension shear as the objective function are denoted by C followed by the corresponding ply count. It is evident by comparing the performance of the S_{12} optimized laminates to the optimized extension shear laminates that the extra stiffness coefficients have only a small effect on the amount of tension torsion response. The four ply laminates yield an identical solution and the five, six, seven, and eight ply solutions yield only a small increase in the value of S_{12}, noted in Figure 3.5.

Table 3.4 Optimal Extension Twist Compliance Laminates and Extension Shear Laminates

# of Plies	**S_{12} Objective Function Sequences**	**S_{12} $(Nm)^{-1}$ x 10^{-6}**
4	[22.5/-67.5/-67.5/22.5]	17.2
5	[29.7/-74.8/-22.5/-74.8/29.7]	3.10
6	[87.62/-14.77/-11.35/56.35/59.76/-42.62]	3.19
7	[62.71/-17.7/-17.7/-67.5/62.73/62.7/-17.7]	3.44
8	[73.1/-22.2/-15.5/65.9/-21.3/69.4/71.3/-21.2]	7.89
	Extension Shear Objective Function Sequences	
4	[22.5/ -67.5/ -67.5/ 22.5]	17.2
5	[29.9/ -74.6/ -22.5/ -74.6/ 29.8]	3.10
6	[88.7/ -9.6/ -15.7/ 60.3/ 54.36/ -44.1]	2.76
7	[37.6/ -17.8/ -74.1/ -71.4/ 33.9/ -62.2/20.1]	2.73
8	[27.7/-60.3/30.3/-61.2/ -62.5/ 27.6/-65.0/25.4]	7.78

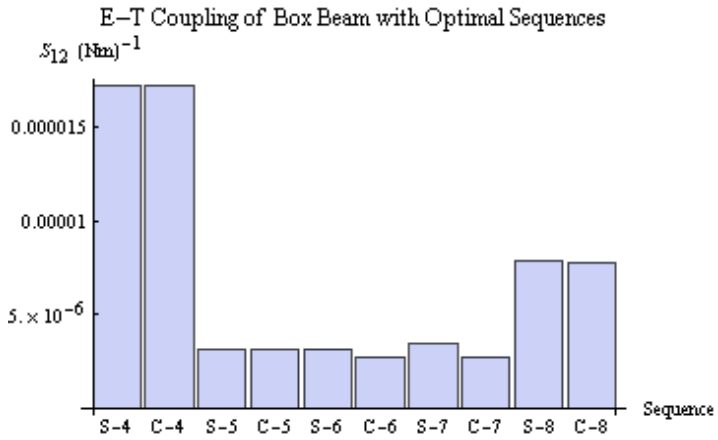

Figure 3.5 S_{12} optimization performance vs. extension shear optimization performance

3.3 Parametric Study

According to the constitutive equation for the closed cell section, the level of coupling is dependent on the area enclosed by the box beam. It is also a recognized fact, noted in Haynes *et al.*[5] work, that the level of coupling decreases in flat strips as the thickness of the strip increases. In order to tailor the stiffness of the beam for the intended application the thickness and enclosed area can be varied. To understand the effect that varying the enclosed area and thickness have on the extension twist coupling a parametric study is conducted.

Due to computational constraints, the closed form solution was used for this study. However, a verification of the accuracy of the closed form solution is shown by Figure 3.6 which compares the VABS finite element solution to the closed form solution for a box beam configuration. The box beam used for the verification study is 15 cm by 5 cm and has 30 degree angle ply orientation in a CUS configuration. The thickness is varied from 0.1mm to 2.5 cm. The VABS and closed form solution follow the same trend for thicknesses that maintain the thin shelled definition of a thickness 10% of the height or width cross sectional dimension and then departs once that ratio is invalid.

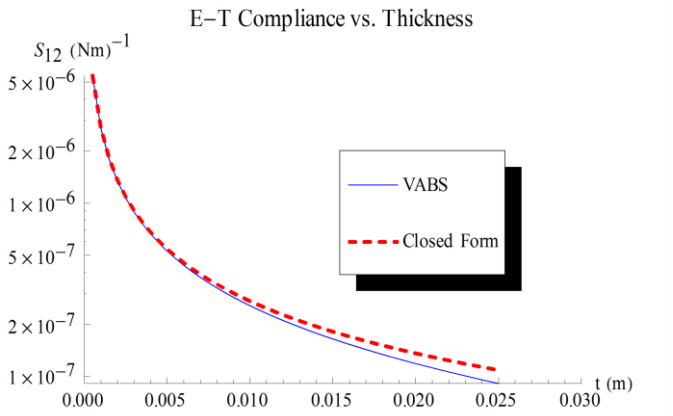

Figure 3.6 VABS and closed form solution comparison

3.3.1 Varying Thickness

It is important to note that this study is intended to illustrate the trends between the thickness and the stiffness of the box beam. Since the stiffness depends entirely on the in-plane stiffness coefficients from classical lamination theory, the thickness has a linear effect on the in-plane stiffness coefficients and can be extracted and used as a parameter. In the following studies base laminates without a set ply thickness are used. This is done for computational efficiency. Although this is an acceptable method of determining the trend between thickness and compliance, there are constraints on the thickness values that can actually be obtained. The actual thickness that can be obtained depends on the material system used. The only way to increase the thickness of the sequence is to increase the number of plies in the sequence.

The thickness of a standard box beam is varied monotonically. The initial thickness is varied from 0.1 mm to 10mm and the height and width dimensions remain constant at 8 cm and 16 cm, respectively. The two base sequences used for the study are the best performing sequences from the current and former optimization routines. The results from the study are illustrated in Figures 3.7, 3.8 and 3.9. Figure 3.7 illustrates that the former approach

outperforms the current approach by an average of 62% for a constant thickness over the range of thickness studied.

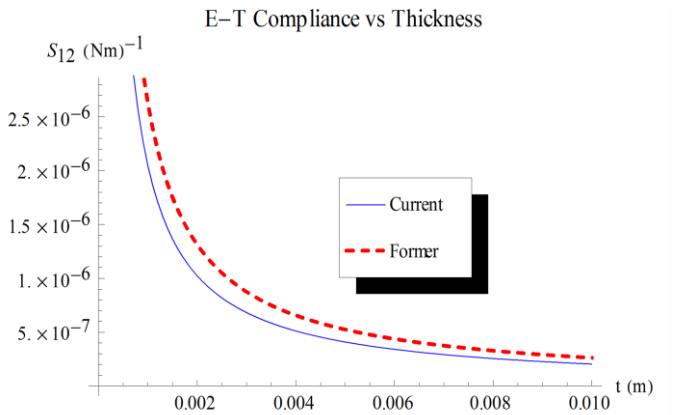

Figure 3.7 Trend between e-t coupling and thickness

Since the design of a structure is generally dependent on the stiffness requirement of the application, the bending (C_{33}) and torsional (C_{22}) stiffness are taken into consideration as well. Figures 3.8 and 3.9 illustrate the trend between stiffness and S_{12} compliance coefficient for the current and former 4 ply base laminates. Figure 3.8 indicates that the 4 ply laminate from the current routine performs 15% better in terms of the extension twist coupling over the range of thickness than the than the 4 ply laminate from the former routine when the bending stiffness is held constant. It should also be noted that the laminate is more material efficient as less material is required to generate the same levels of bending stiffness and extension twist coupling. This is realized by noting that the trend from the current laminate extends further into higher stiffness levels and the fact that the thickness range was the same for both of the laminates. This suggests that depending on the stiffness requirements of a particular design goal, it may be more advantageous to optimize the laminates for extension twist coupling while taking into consideration the stiffness requirements. More light is shed on this revelation in chapter 4. Figure 3.9 indicates that when the torsional stiffness is held constant the former

approach performs better as higher levels of extension twist coupling correspond to the same level of torsional stiffness.

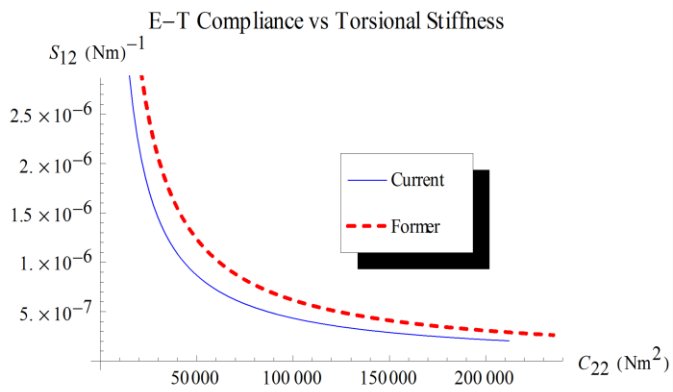

Figure 3.8 Vary thickness case- Trend between e-t compliance and bending stiffness

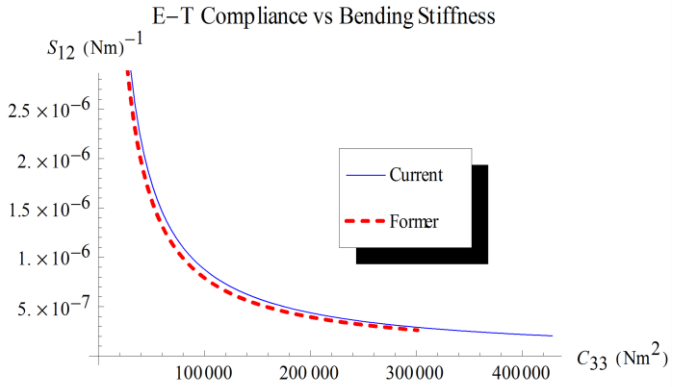

Figure 3.9 Varying thickness case- Trend between e-t compliance and torsional stiffness

3.3.2 Varying Area

To maintain a consistent geometric shape the area of a box beam illustrated in Figure 3.10 is varied monotonically by increasing the height and width by a consistent factor. The thickness of the section remains constant. In order to analyze the performance of the current approach and the previous approach, the 4 ply laminates from each optimization routine are compared.

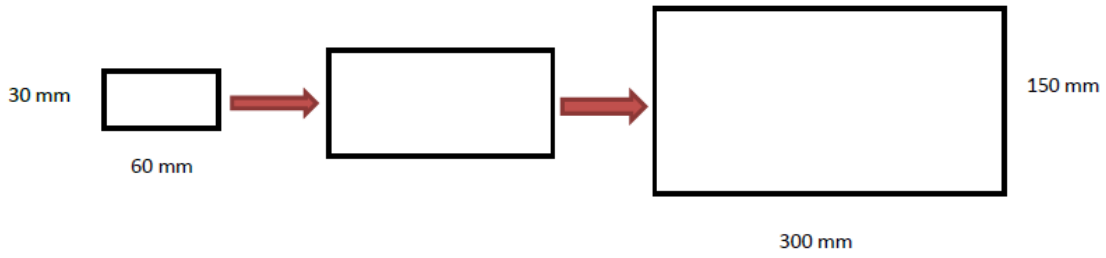

Figure 3.10 Initial and final box beam dimensions

Noted by Figure 3.11 the former approach produces and average of over 35% higher levels of extension twist coupling than the current approach throughout the range of areas. Figures 3.12 and 3.13 plot the extension twist compliance coefficient S_{12} against the bending and torsional stiffnesses.

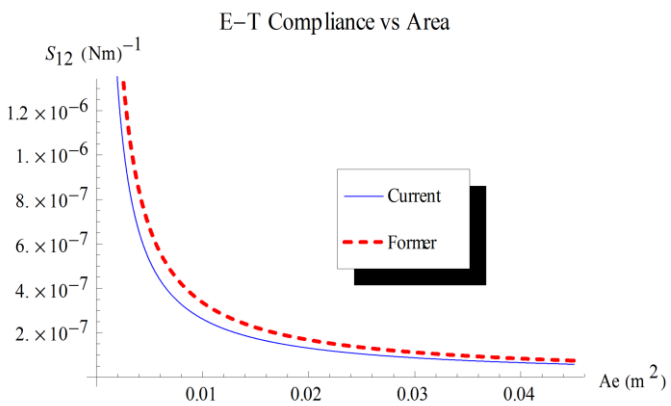

Figure 3.11 Trend between e-t compliance and area

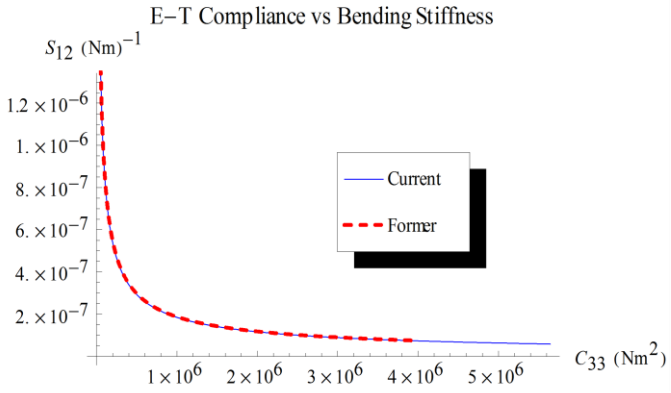

Figure 3.12 Trend between e-t compliance and bending stiffness

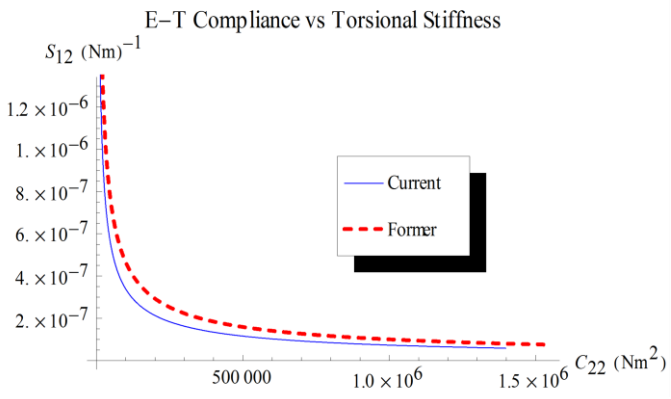

Figure 3.13 Trend between e-t compliance and torsional stiffness

The results demonstrate that, although there exists a significant difference between the level of coupling between the current and former approach when the area remains the same, the difference between the level of coupling when the bending stiffness is held constant is minimal. This occurs because the ratio between the level of coupling and the bending stiffness is similar for both laminates. In other words, the former laminate yields a level of extension twist coupling higher for a given area, but the current laminate yields a higher bending stiffness for a given area. Thus, the current laminate can produce nearly the same level of coupling and stiffness for a box beam with a smaller area than the former laminate. This demonstrates the material efficiency of using the current laminates over the former, since not as much material is required to generate the same levels of stiffness and compliance as the former laminate. The trends between E-T compliance and torsional stiffness for the laminates are similar to the varying thickness case, as the former laminate yields a trend that is better than the current laminate.

3.4 Hygrothermal Stability

The hygrothermal stability requirement of the current optimization routine guarantees zero out of plane warping in flat strip configuration due to a thermal or hygral change. This,

however, does not guarantee hygrothermal stability in box beam configuration. This is due to the fact generated by opposing shear deformation in material with respect to the mid plane of the section that the mechanism for induced twisting in closed cell configuration depends on the continuity of shear flow. Since the hygrothermally stable optimized laminates do not guarantee zero thermally induced shear deformation, a moment and a resulting twist deformation can be induced by a temperature change in a box beam with the laminates in CUS configuration. The extent that a thermal environment will have an effect on the hygrothermal stability of the box beam is considered.

The level of thermal coupling is quantified by the induced twist rate in the box beam when it is subject to a temperature change of 50° C. Three separate studies are conducted. The first is a direct comparison between the thermal coupling present in a box beam with the current and former (Lentz[9]) optimal laminates. The second and third studies are parametric studies in which the thickness and the area of the box beam are variables.

3.4.1 Direct Comparison

A direct comparison of the thermal induced twist rate in the current and former optimal laminates introduced into a box beam with the same dimensions is shown in Figure 3.3. The base 4 ply sequences from the former and current approach are denoted by an L and C, respectively, followed by the corresponding ply number. The thermal analysis was conducted in the VABS software. It is evident from the results in Figure 3.14 that the current approach produces laminates that have thermally induced twist that is close to zero for all the laminates. The former approach laminates produce twist rates that are more than 1.5 degrees per meter.

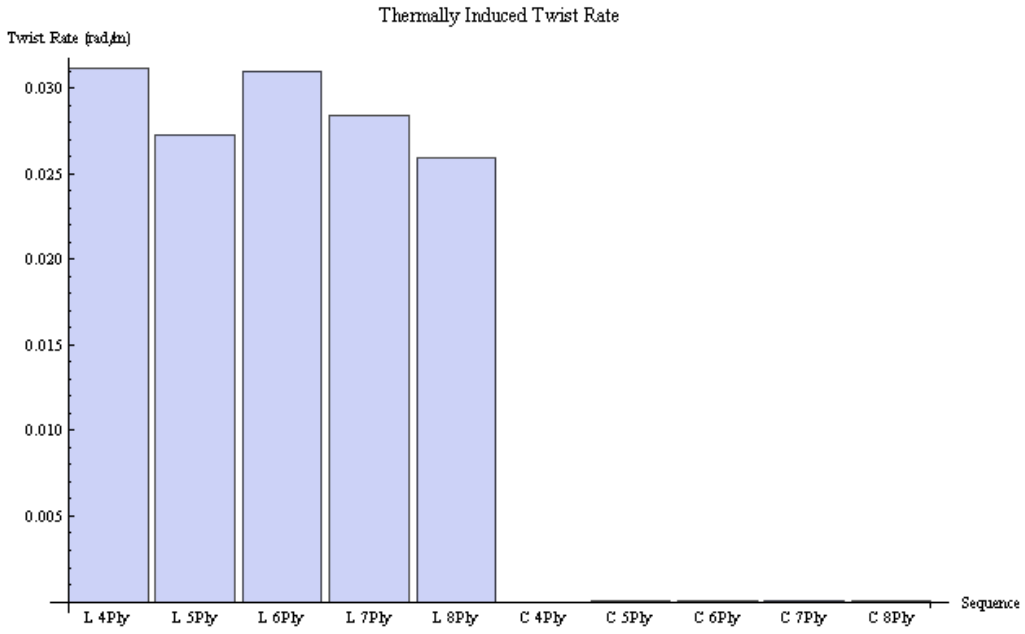

Figure 3.14 Thermal coupling comparison current vs. Lentz *et al.*[9]

3.4.2 Parametric Comparison

In order to fully analyze the effect that a thermal environment has on the amount of induced twist, a parametric study is conducted in which the enclosed area and thickness of the box beam are varied. The 4 ply sequences from the former and current optimization routines are used for comparison in the study.

3.4.2.1 Varying Thickness

The thickness of a box beam with the height and width dimensions of 5 cm and 15 cm, respectively, was varied from a thickness of 0.1 mm to 1 cm. The thermal induced twist rate was recorded for each thickness and the results for the 4 ply laminates from both approaches are plotted in Figure 3.15. The trend as the thickness increases is most closely linear and does not vary significantly for both laminates. The exact reasoning for the opposite trend of the two laminates has not been fully investigated. However, a convergence study was conducted, which eliminated the possibility of the necessity of mesh refinement as the trends remained the

same as the number of nodes is increased. The thermally induced twist in the former approach as thickness is varied is higher with a range of thermally induced twist rate from 0.04 rad/m to 0.03 rad/m.

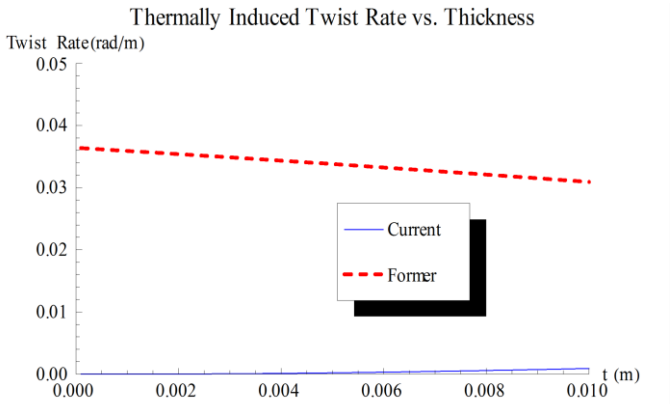

Figure 3.15 Thermally induced twist rate with thickness variation

3.4.2.2 Varying Area

The area of a box beam is varied monotonically by increasing the height and width dimensions by 25%. The initial size of the box beam is 1.5 cm by 0.5 cm and the final size is 33 cm by 11 cm. The results in Figure 3.16 indicate that there is a drop off in the level of thermally induced twist when the area of the box beam is initially increasing and then once the cross sectional area increases, there are less significant changes in the thermally induced twist. This likely occurs because the ratio between perimeter and area noted in the closed form solution for torsional stiffness is greater when the box beam area is smaller. As the torsional stiffness increases the influence that a thermal change has on the box beam is reduced. This result suggests that for smaller box beams the hygrothermal stability may become compromised for the current approach. This effect should be taken into consideration when the designing elastically tailored closed cell structures. As the area increases beyond 0.001 m^2 the current laminate proves to be more hygrothermally stable than the former laminate as the twist rate approach levels that are very small.

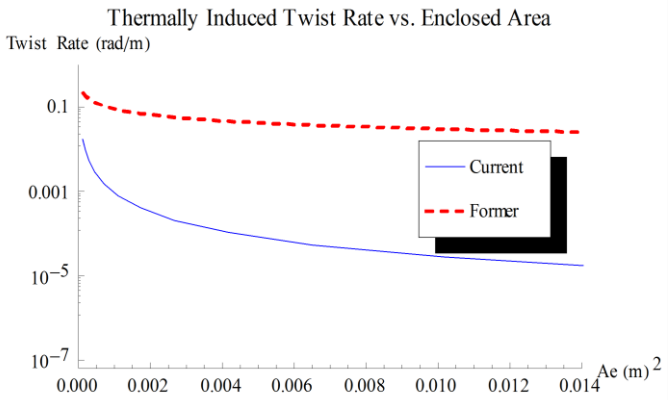

Figure 3.16 Thermally induced twist rate with area variation

CHAPTER 4

OPTIMAL SEQUENCES WITH STIFFNESS CONSIDERATION

Most structural applications require high levels of stiffness in one or two directions but may not need equivalently as high levels of stiffness in the other directions. This concept is well understood and has been implemented into structural design for many years. In fact, the fundamental advantages of composite materials result from this concept. This suggests that the optimization of laminate stacking sequences should not only focus on one stiffness term. Rather, it should take into consideration all of stiffness requirements of the application that the laminate will be applied to.

The results from the parametric study that plot the level of extension twist coupling vs. the stiffness values demonstrate the potential of optimizing the laminates for S_{12} compliance and the desired stiffness. The objective function in optimization routine utilized in previous optimizations is altered to yield a more positive relationship between extension twist and stiffness. Namely the goal is to generate laminates that exhibit high levels of stiffness and extension twist coupling. The objective function is obtained by taking the product of the desired stiffness and compliances. This effectively maximizes the trend between compliance and stiffness. A symbolic form of the objective function is noted in Eq. 4.1.

$$F = \left[Desired\ Stiffness\ Coefficient \times Desired\ \ Compliance\ Coefficient \right] \qquad [4.1]$$

Since the focus of this study is on extension twist coupling in closed cell sections, the optimization will be performed for coupled levels of bending stiffness and extension twist compliance as well as torsional stiffness and extension twist compliance.

4.1 Bending Stiffness and Extension Twist Compliance

In a CUS box beam the level of bending stiffness is largely governed by the primary in-plane extensional stiffness coefficient A_{11} from the stiffness matrix derived by classical lamination theory. This is evident by noting the dominance of the reduced axial stiffness coefficient denoted by A in the bending stiffness Eq. 4.2 derived from the variational asymptotic anisotropic beam theory for a box beam. The reduced axial stiffness equation is also referenced for convenience.

$$C_{44} = 2\left(A - \frac{B^2}{C}\right)\left(\frac{1}{12}W^3 + \frac{1}{4}W^2 H\right) \qquad A = A_{11} - \frac{A_{12}^2}{A_{22}} \qquad [4.2]$$

H and W are representative of the height and width of the beam and A, B, and C are the reduced axial, coupling, and shear stiffnesses [Eqs. 1.9-1.11], respectively. It is undeniable that the reduced coupling and shear stiffness take a role in level of bending stiffness as well. For this reason the optimization will consider all of the terms in the bending stiffness and extension twist compliance equation. The objective function for the optimization is listed in Eq. 4.3.

$$F = S_{12} \times C_{44} \qquad [4.3]$$

The results from the optimization for 4 to 8 plies are listed in Table 4.1. Figure 4.1 plots the value of extension twist compliance as the thickness varies from 0.1mm to 1 cm and the height and width of the box beam remain constant at 8cm and 16 cm. The sequences are denoted by a B followed by the corresponding ply number. Note that the B4 and B8 sequences outperform the other sequences and display nearly the same trend. The nearly identical trend is a result of the values in-plane stiffness coefficients (thickness extracted) being in close proximity. Figure 4.2 plots the extension twist compliance value for areas in the range 1.8×10^{-3} m^2 to 45×10^{-3} m^2 and the ply thickness is held constant at 0.152 mm.

Table 4.1 Coupled Bending Stiffness and E-T Compliance Optimized Laminates

Plies	Stacking Sequence
4	[77.5 / -12.5 / -12.5 / 77.5]
5	[64.2 / -11.4 / -63.6 / -11.4 / 64.1]
6	[52.0/ -25.6 / -29.0 / 83.3 / 79.8 / 2.2]
7	[68.2 / -12.2 / -12.2 / -62.0/ 68.10 / 68.2 / -12.2]
8	[77.5 / -12.5 / -12.5 / 77.5 / 77.5 / -12.5 / -12.5 / 77.5]

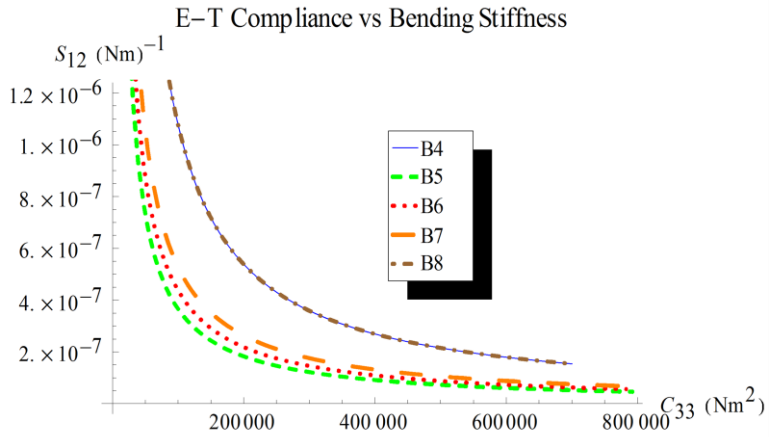

Figure 4.1 Trend between e-t compliance and bending stiffness for the coupled optimization laminates as thickness varies

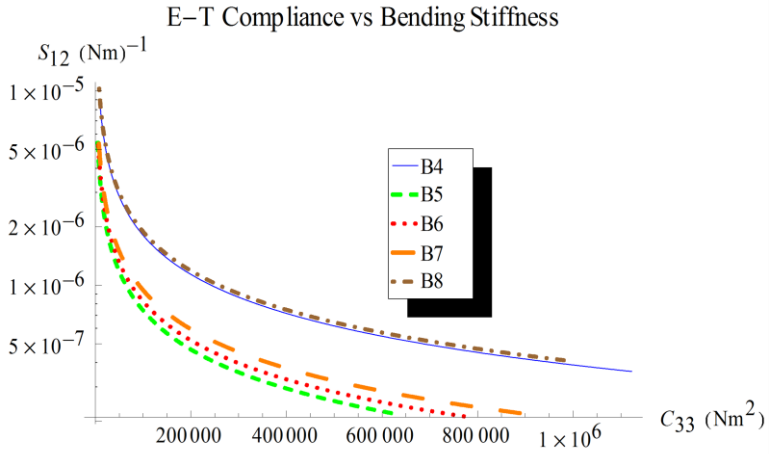

Figure 4.2 Trend between bending e-t compliance and stiffness for the coupled optimization laminates as area varies

4.1.1 Comparison of the Optimization Routines

In the previous parametric analysis of the trends between extension twist compliance and stiffness, the improvement in the trend is only noted and the constraints on the actual thicknesses attainable are not taken into consideration. In order to make a more realistic comparison between the optimization routines, the constraint on the actual thickness obtainable is taken into consideration.

The three laminates chosen for comparison in the routine are the 4 ply laminate from the Lentz[9] optimization, the extension shear optimization, and the optimization for the trend between bending stiffness and compliance. Table 4.2 lists the laminates that are compared. The coupled optimization routine is denoted by B4 and the optimization routines referred to as the current and former routines in Chapter 3 are denoted by C4 and L4, respectively.

Table 4.2 Four Ply Laminates for Comparison

Optimization Routine	**Stacking Sequence**
Lentz[9] (L4)	[-81.8 / -81.8 / 30.5 / 30.5]
Extension Shear (C4)	[-67.5 / 22.5 / 22.5 / -67.5]
Coupled Bending Stiffness and E-T coupling (B4)	[77.5 / -12.5 / -12.5 / 77.5]

The laminates are introduced into a CUS box beam configuration and the trend between E-T compliance and bending stiffness are evaluated for a varying thickness and varying area case. For the varying thickness case, the thickness is varied more realistically by increasing the number of plies in the base 4 ply stacking sequence as shown in Eq. 4.4, where $\theta 1$- $\theta 4$ are the ply orientations of the corresponding optimal sequence and *n* is the parameter that is varied. The dimensions of the box beam remain 0.08 m x 0.16 m.

$$\left[\theta 1_n / \theta 2_n / \theta 3_n / \theta 4_n\right] \qquad [4.4]$$

For the varying area case the laminates maintain a constant ply thickness of 0.0762 mm and the dimension of the box beam is varied from 3 mm x 6 mm to 15 cm x 30 cm.

Figures 4.3 and 4.4 compare the performance of the laminates from the separate optimization routines. For varying thickness the trend between bending stiffness and extension twist is improved by 40% from the L4 sequence to the B4 sequence. Also notice that the trend for the B4 laminate from this optimization extends further into higher levels of stiffness. Since the range of thickness and area is constant for the three laminates considered, this indicates that less material is required to produce the same level of stiffness and coupling compliance.

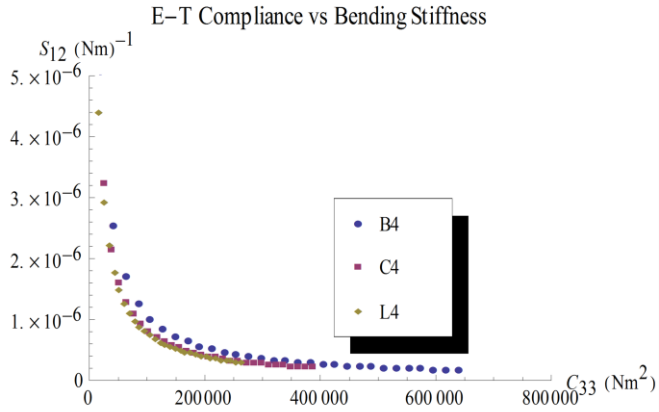

Figure 4.3 Trend between e-t compliance and bending stiffness for the four ply base laminates from each optimization routine as the thickness varies.

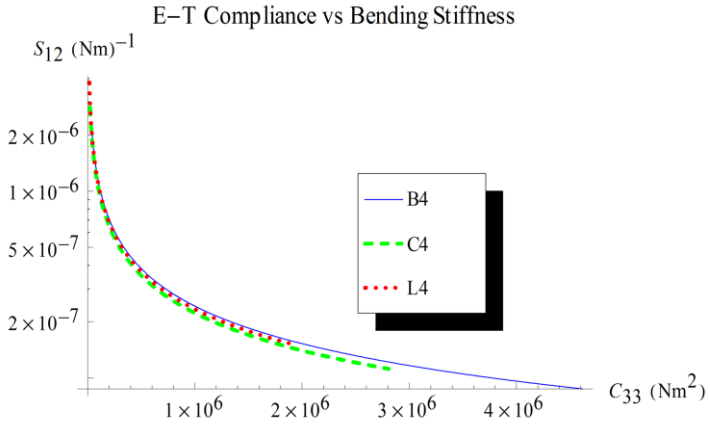

Figure 4.4 Trend between e-t compliance and bending stiffness for the four ply base laminates from each optimization routine as the area varies.

In order demonstrate the advantage of using a stacking sequence that is optimized for the trend between extension twist compliance and stiffness, the bending stiffness and thickness of box beams with the B4 and L4 laminates having similar levels of coupling are compared in Table 4.3. For all the cases the amount of material required to generate the same level of coupling in the B4 laminate is close to 40% less than material required for the L4 laminate. In addition to the material efficiency improvement, the level of bending stiffness is more than 20% higher for all the cases and improves to 40% for thicker beams.

Table 4.3 Comparison of Sequences with Similar Levels of Coupling

Sequences	**E-T Compliance**	**Thickness**	**Stiffness**
[12.85 / -77.15 / -77.15 / 12.85]	$2.53\ 10^{-6}$	.608	42.6
$[-81.84_2 / -81.84_2 / 30.48_2 / 30.48_2]$	$2.20\ 10^{-6}$	1.216	35.1
Percent Difference	**15%**	**-50%**	**21.4%**
$[12.85_2 / -77.15_2 / -77.15_2 / 12.85_2]$	$1.26\ 10^{-6}$	1.216	85.1
$[-81.84_4 / -81.84_4 / 30.48_4 / 30.48_4]$	$1.10\ 10^{-6}$	2.432	70.2
Percent Difference	**14.5%**	**-50%**	**21.2%**
$[12.85_3 / -77.15_3 / -77.15_3 / 12.85_3]$	$8.43\ 10^{-7}$	1.824	127.7
$[-81.84_5 / -81.84_5 / 30.48_5 / 30.48_5]$	$8.80\ 10^{-7}$	3.04	87.8
Percent Difference	**-4.2%**	**-40%**	**45.4%**
$[12.85_4 / -77.15_4 / -77.15_4 / 12.85_4]$	$6.32\ 10^{-7}$	2.432	170.3
$[-81.84_7 / -81.84_7 / 30.48_7 / 30.48_7]$	$6.28\ 10^{-7}$	4.256	122.9
Percent Difference	**0.6%**	**-42.9%**	**38.6%**
$[12.85_5 / -77.15_5 / -77.15_5 / 12.85_5]$	$5.06\ 10^{-7}$	3.04	212.9
$[-81.84_9 / -81.84_9 / 30.48_9 / 30.48_9]$	$4.89\ 10^{-7}$	5.47	158.0
Percent Difference	**3.4%**	**-44.4%**	**34.7%**
$[12.85_6 / -77.15_6 / -77.15_6 / 12.85_6]$	$4.22\ 10^{-7}$	3.64	255.0
$[-81.84_{10} / -81.84_{10} / 30.48_{10} / 30.48_{10}]$	$4.40\ 10^{-7}$	6.08	175.3
Percent Difference	**-4.3%**	**-40.1%**	**45.5%**
$[12.85_7 / -77.15_7 / -77.15_7 / 12.85_7]$	$3.61\ 10^{-7}$	4.256	298.0
$[-81.84_{12} / -81.84_{12} / 30.48_{12} / 30.48_{12}]$	$3.66\ 10^{-7}$	7.296	210.7
Percent Difference	**-1.4%**	**-41.6%**	**41.4%**
$[12.85_8 / -77.15_8 / -77.15_8 / 12.85_8]$	$3.16\ 10^{-7}$	4.864	340.6
$[-81.84_{13} / -81.84_{13} / 30.48_{13} / 30.48_{13}]$	$3.38\ 10^{-7}$	7.904	228.3
Percent Difference	**-7.0%**	**-38.4%**	**49.2%**

4.2 Torsional Stiffness and E-T Compliance

An inverse relationship between torsional stiffness and extension twist coupling compliance in closed sections has been identified in past work[15]. This relationship has been proven to be quite restrictive for generating high levels of torsional rigidity and extension twist compliance simultaneously.

In order to optimize for the trend between extension twist compliance and torsional stiffness, the objective function used for the optimization is identified in Eq. 4.5. The optimization routine was performed for 5 laminates with ply count varying from 4 to 8. The results from the optimization routine are listed in Table 4.4. Figures 4.5 and 4.6 plot the S_{12} compliance coefficient vs. the C_{22} stiffness coefficient over a range of thicknesses and areas for the laminates obtained from the optimization. The sequences are denoted by a T followed by the corresponding ply number. The trend for the 4 ply laminate substantially outperforms the other laminates. This is consistent with the superior results of the 4 ply laminate in the coupled bending stiffness and extension twist compliance optimization.

$$F = S_{12} \times C_{22} \qquad [4.5]$$

Table 4.4 Coupled Torsional Stiffness and E-T Compliance Optimized Laminates

Plies	**Stacking Sequence**
4	[59.2 / -30.8 / -30.8 / 59.2]
5	[55.3 / -20.2 / -72.5 / -20.2 / 55.3]
6	[41.8 / -35.8 / -39.2 / 73.1 / 69.6 / -8.0]
7	[56.5 / -23.9 / -23.9 / -73.7 / 56.5 / 56.5 / -23.9]
8	[39.1 / -32.2 / 71.0 / -35.3 / -39.0 / 66.7 / 66.7/-6.8]

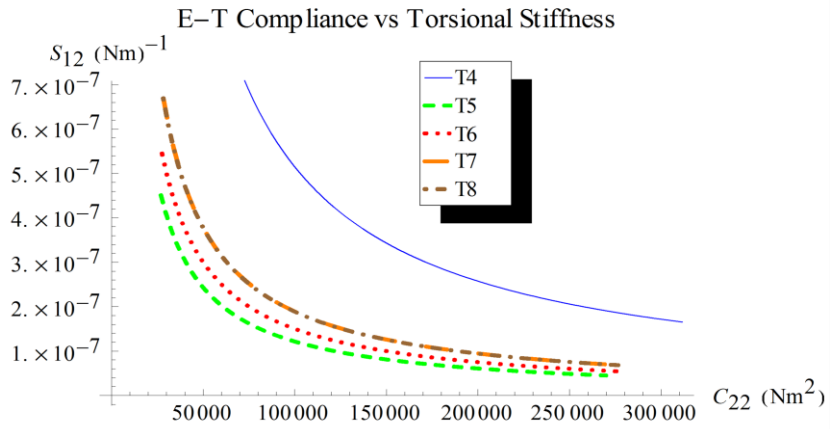

Figure 4.5 Trend between e-t compliance and torsional stiffness for the four ply base laminates from each optimization routine as the thickness varies.

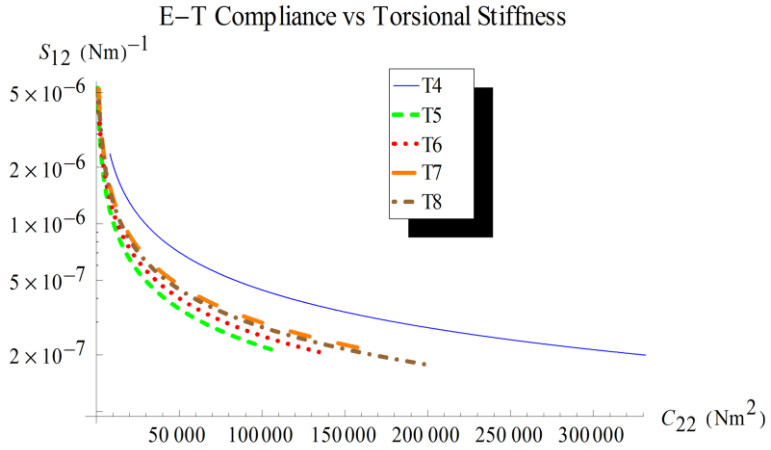

Figure 4.6 Trend between e-t compliance and torsional stiffness for the four ply base laminates from each optimization routine as the area varies.

4.2.1 Comparison of the Optimization Routines

The trends between extension twist compliance and torsional stiffness are compared for the three optimization routines. The four ply laminate from each routine are chosen for comparison and listed in Table 4.5. The Lentz optimization, extension shear optimization, and coupled torsional stiffness and extension twist coupling optimizations are denoted by, L4, C4, and T4, respectively.

Table 4.5 Optimal Four Ply Laminates for Comparison

Optimization Routine	Stacking Sequence
Lentz[9] (L4)	[-81.8 / -81.8 / 30.5 / 30.5]
Extension Shear (C4)	[-67.5 / 22.5 / 22.5 / -67.5]
Coupled Torsional Stiffness and E-T coupling (T4)	[59.2 / -30.8 / -30.8 / 59.2]

The thickness is varied more realistically using Eq. 4.4 and varying the parameter *n.* Figures 4.7 and 4.8 show that there is a 31% improvement in trend between torsional stiffness and extension twist compliance for the T4 laminate when compared to the C4 laminate. The constraint on hygrothermal stability has a larger effect on the level of coupling and torsional stiffness than the level of coupling and bending stiffness as the trend for the laminate from the former routine (L4) is 14% better than the trend for the laminate from the coupled optimization routine (T4).

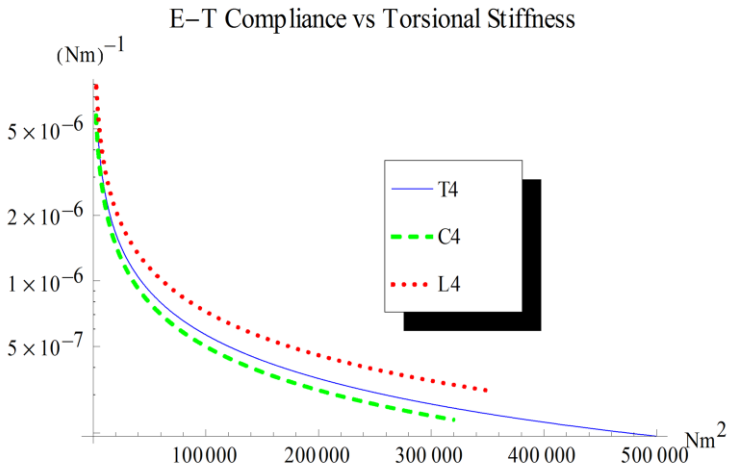

Figure 4.7 E-T compliance vs torsional stiffness for the four ply base laminates as area varies

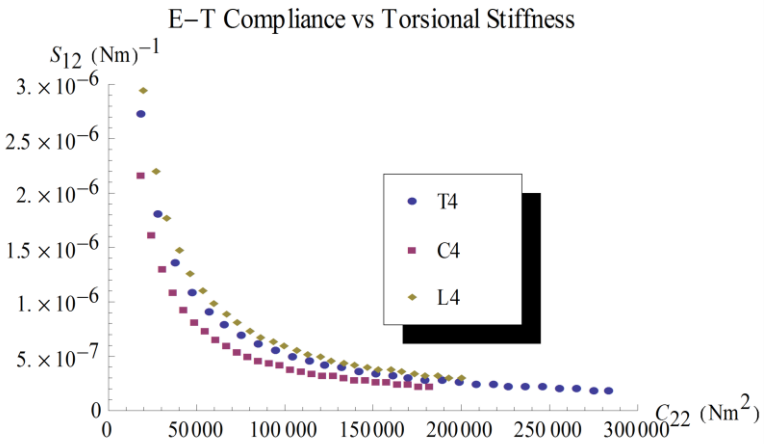

Figure 4.8 E-T compliance vs. torsional stiffness for the four ply base laminates as thickness varies

CHAPTER 5

XV-15 TILT ROTOR CASE STUDY

To evaluate the feasibility of using the optimal sequences for passive blade control, a low level design optimization is performed on a blade section of an XV-15 tilt rotor in which only the level of stiffness is taken into consideration. A representative airfoil section with constraints on stiffness is defined and the level of coupling attainable is evaluated.

The tip of the blade experiences the highest aerodynamic and inertial loads and is the most effective region for passive blade control. In addition, the levels of stiffness in this region are not nearly as constraining to passive blade control as the stiffness requirements near the root of the blade. Work conducted by Ozbay[15] suggested the required levels of stiffness as a function of the blade span. The stiffness requirements for the .8r to 1r region, where r is non-dimensional blade span, are listed in Table 5.1.

Table 5.1 Stiffness Requirements for the 80% Span to Blade Tip Region

Stiffness Type	**Stiffness**
Chord-wise Bending Stiffness (EI)	500 kN-m^2
Flap-wise Bending Stiffness (EI)	20 kN-m^2
Torsional Stiffness (GJ)	30 kN-m^2

5.1 Design of Blade Section

A model for a NACA0012 airfoil has been generated for analysis in VABS. The preprocessor generating the geometry and mesh was written in Mathematica. The mesh generated has over 4,000 elements and 70,000 degrees of freedom. Since the required level of torsional stiffness is much lower in the blade tip region, a D spar without a web section is chosen. The chord length of the section was chosen to be 0.35 m.

To generate a model that fit the stiffness constraints the thickness was increased by using Eq. 4.4 and varying the *n* parameter to define the sequence for the airfoil section until all of the stiffness requirements were met. For simplicity the D-spar section had a constant thickness of 7.904 mm. The material constants from the material system T-300-976 Graphite/Epoxy were used and provided in Table 5.2. The stacking sequences obtained from the optimizations that coupled high stiffness with extension twist coupling were used. The optimizations were updated with the proper material constants. In addition, a third stacking sequence is obtained from defining an objective function that takes into consideration both the bending and torsional stiffness requirements.

Table 5.2 Material Properties of T-300-976 Graphite/Epoxy

Moduli of Elasticity	**Shear Moduli**	**Poisson's Ratio**	**Ply Thickness**
E_{11} = 125 GPa	$G_{12} = G_{13}$ = 4.3 GPa	$\upsilon_{12} = \upsilon_{13} = \upsilon_{23}$ =0.328	tp = 0.152 mm
$E_{22} = E_3$ = 8.45 GPa	G_{23} = 3.4 GPa		

The third stacking sequence was designed to be a compromise between the optimal sequences for the best trend between extension twist and bending stiffness and extension twist and torsional stiffness. The C_{33} and C_{22} terms are normalized by dividing the resulting stiffness value by the maximum value. The value denoted by the max subscript is obtained by maximizing the sequences for the corresponding stiffness individually. Note that this is not necessary when taking into consideration only one stiffness value and the compliance value S_{12}. However, because the stiffness C_{22} and C_{33} may have different magnitudes relative to each other, one of the values may be naturally dominant over the other. Avoiding this step would likely produce sequences that would favor one of the stiffnesses. The objective function is shown in Eq. 5.1.

$$F = -\left(\frac{C_{33}}{C_{33\max}}\right)\times\left(\frac{C_{22}}{C_{22\max}}\right)\times\left(\frac{S_{12}}{S_{12\max}}\right) \qquad [5.1]$$

5.2 Twist Requirements

The magnitude of passive twist curvature required for optimal performance for the XV-15 rotor was suggested in Ozbay's[15] work to be 11 degrees per 50 % of the blade span. From this it can be reasonably assumed that the target twist rate for the 20% of the span is approximately 4.4 degrees.

The magnitude of centrifugal force experienced by the blade in the tip region is calculated by integrating Eq. 5.2, defining centrifugal force, from 0.8 r to r. Where, ω is the angular velocity of the blade, m_r is the mass per unit span, and x is the distance from the root of the blade. In hover and forward flight mode the angular velocities are 59.2 rad/s and 48 rad/s, respectively. The difference between the forces calculated in the two regimes is assumed to be the variation in axial force that can be utilized for passive blade control.

$$Fc = \int_{0.8r}^{r} \omega^2 m_r x \quad dx \qquad [5.2]$$

It is important to note that the blade experiences additional loads that can have parasitic effects on the amounts of induced twist resulting in the blade. For simplicity and since this study is intended to illustrate the importance of the stacking sequence in the design process, the additional loads on the blade are not taken into account.

5.3 Results

The thicknesses meeting the stiffness requirement for the airfoil section and D spar section for the three optimal sequences are shown in Table 5.3. The stiffness, extension twist compliance and twist achievable values are listed in Table 5.4.

Table 5.3 Geometric Properties Meeting the Stiffness Requirements

Optimization	Stacking Sequence- D-spar, Airfoil	Mass Per Unit Span (Kg/r)	Thickness of D-spar (mm)	Thickness of Airfoil (mm)
Torsional Stiffness	$[59.3_{13}/\text{-}30.7_{13}/\text{-}30.7_{13}/59.3_{13}]$ $[59.29_{6}/\text{-}30.71_{6}/\text{-}30.71_{6}/59.29_{6}]$	6.70	7.904	3.648
Torsional and Bending Stiffness	$[63.7_{13}/\text{-}26.3_{13}/\text{-}26.3_{13}/63.7_{13}]$ $[63.72_{5}/\text{-}26.28_{5}/\text{-}26.28_{5}/63.72_{5}]$	6.04	7.904	3.04
Bending Stiffness	$[77.2_{13}/\text{-}12.8_{13}/\text{-}12.8_{13}/77.2_{13}]$ $[77.2_{9}/\text{-}12.8_{9}/\text{-}12.8_{9}/77.2_{9}]$	8.64	7.904	5.472

Table 5.4 Predicted Stiffness and Twist Variation

Optimization	Torsional Stiffness (kN-m^2)	Flap-wise Bending Stiffness (kN-m^2)	Chord-wise Bending Stiffness (kN-m^2)	Extension Twist Compliance ((Nm)$^{-1}$)	Twist Variation (Deg)
Torsional Stiffness	42.1	20.9	785	3.02 E-7	3.65
Torsional and Bending Stiffness	30.2	20.7	808	4.08 E-7	4.46
Bending Stiffness	30.9	71.8	2448	2.09 E-7	3.26

The results from this case study illustrate the importance of the selection of the stacking sequence. The first thing that should be noted from the case study is the stacking sequences resulting from the optimization routines used. The three sequences used maximize the trend between extension twist coupling and torsional stiffness, bending stiffness, and combined bending and torsional stiffness. The resulting sequences are all variations of the Winckler-type sequence, as they are identically half of a Winckler-type sequence $[\theta/(\theta-90)_2/\theta/-\theta/(\theta-90)_2/-\theta]$. It can also be inferred from investigating the sequences that there exists a range from the best trend between extension twist compliance and torsional stiffness to the best trend between extension twist compliance and bending stiffness. Ideally this range can be used as a parameter in the design process. For example, if the bending stiffness is the most difficult stiffness to accomplish in a given structural configuration, choosing θ near the 77 degree orientation would be the most ideal for the application. The reason this type of design approach is successful when designing applications for extension twist coupling is that it allows for the thickness of the laminates to be reduced. Due to the negative

relationship between thickness and extension twist coupling, this not only increases the material efficiency of the application but also allows for higher levels of extension twist coupling.

The best performing laminate in terms of the predicted twist variation was the laminate optimized for coupled bending stiffness, torsional stiffness, and extension twist compliance. It produced an estimated twist variation of 4.46 degrees, and it meets the predicted twist variation necessary for the maximum performance improvement in the tilt-rotor in the 80% span to blade tip region. The configuration with this stacking sequence is also the thinnest sequence, which further demonstrates the importance of the layup and the inverse relationship between thickness and extension twist compliance. Examination of the stiffness results from the other two sequences further demonstrates the importance of the selection of the sequence. The bending stiffness optimal sequence produces levels of bending stiffness in the airfoil configuration that far exceed the required amounts for the application. The reason that the bending stiffness is higher is due to the necessity of increasing the thickness to increase the torsional stiffness to the required level. This is an example of an inefficient use of the material. The optimal torsional stiffness sequence is not nearly as material inefficient as the bending stiffness sequences, but still had room for improvement, as the torsional stiffness was more than 30% higher than necessary.

This design approach only used three of the stacking sequences in the suggested range for optimal extension twist coupling and stiffness. A better design approach would be to find the best laminate in the range suggested for the application. This laminate chosen should be the one that meets the minimum requirements for all the required stiffnesses and as a result will be the thinnest and produce the highest level of coupling.

CHAPTER 6

CONCLUSIONS AND SUGGESTED WORK

This study introduces optimal hygrothermally stable stacking sequences for extension twist coupling in closed cell CUS configuration. The level of coupling achievable by the sequences defined is not superior to the level of coupling achievable in the former optimization routing provided by Lentz[9]. However, when taking into consideration stiffness, the new hygrothermally stable optimized laminates perform better in some cases than the former optimized laminates. An alternative optimization approach which takes into consideration the desired stiffness yields laminates that produce results that are better than the former optimization routine. The trend between bending stiffness and extension twist coupling is improved by 40% using this routine. The material efficiency of the laminates produced is also evident as similar levels of stiffness and coupling correspond to thinner laminates.

The parametric study in this work illustrates the importance of maintaining thin laminates in closed cell configuration to preserve high levels of extension twist coupling as the level of coupling reduces as a function of the inverse of the thickness and the stiffness increases as a function of the thickness. It also suggests that this inverse relationship between thickness and extension twist coupling increases the importance of the stacking sequences used in the closed cell configuration.

The case study on the feasibility of implementing passive blade control through extension twist coupling further demonstrates the importance of the stacking sequence chosen for the configuration. Optimizations that take into consideration the trends between the stiffness and compliance effectively reduce the amount of material required for the application and simultaneously allow for higher levels of coupling. The importance of choosing the stacking

sequence is demonstrated by this work. Proper selection of the sequence allows for thinner laminates and corresponding higher levels of coupling. Since the case study in this work is intended to demonstrate the importance of the stacking sequence on the level of coupling achievable, the design routine demonstrated in this work only takes into account the stiffness requirements of the application. It is undeniably important however, that failure analysis be taken into consideration in the design process. It is also important to understand that the sequences may produce additional couplings. A more comprehensive study which takes into account failure and deformation associated with additional couplings would provide an accurate indication of the feasibility of implementing passive blade control in the tip region.

Equally important to the material comprising the blade is the structure of the blade itself. Developing structures that generate high levels of stiffness while maintaining relatively thin laminates in their configuration has potential for improving the coupling levels between deformation modes. Also, it may also be advantageous to implement other couplings into the structure of the blade that can passively induce twisting. Investigation of combined extension and bend twist coupling is recommended.

The optimizations in this study yield results that are hygrothermally stable in strip configuration. However, it is noted that this does not guarantee hygrothermal stability when the laminates are introduced into box beam configuration because thermally induced shear deformation is not required to be zero. An optimization which constrains the hygrothermally induced shear deformation as well as the curvature in flat strip configuration would ensure hygrothermal stability in box beam configuration.

REFERENCES

[1] Jones, R.M., 1999. Mechanics of Composite Materials, Taylor and Francis, PA, USA.

[2] Krone, N. J. Jr., 1975 "Divergence Elimination with Advanced Composites," AIAA paper, 75-1009, August.

[3] Weisshaar, Terrence A., 1980. "Divergence of Forward Swept Composite Wings," Journal of Aircraft, V 17, n6, p 442-448.

[4] Nixon, M.W., 1988. "Improvements to Tilt Rotor Performance through Passive Blade Twist Control," NASA Technical Memorandum, TM-100583.

[5] Haynes, R.A., Carey, R., and Armanios, E.A., 2009. "A New Class of Hygrothermally Stable Laminates with Extension-twist Coupling," presented at the AHS 65th Annual Forum & Technology Display, May 27-29.

[6] Haynes, R.A, Armanios, E.A., 2010. "New Families of Hygrothermally Stable Composite Laminates with Optimal Extension-twist Coupling," *AIAA Journal,* 48(12): 2954-2961.

[7] Armanios, E. A., Makeev, A., Hooke, D. A., 1996. "Finite Displacement Analysis of Laminated Composite Strips with Extension-Twist Coupling", Journal of Aerospace Engineering, Vol. 9, No. 3, July 1996, pp. 80-91.

[8] Winckler, S.J., 1985, "Hygrothermally Curvature Stable Laminates with Tension-torsion Coupling," Journal of the American Helicopter Society, Vol. 31 (7).

[9] Lentz, W.K., and E.A. Armanios, 1998. "Optimum Coupling in Thin-Walled Closed-Section Composite Beams," Journal of Aerospace Engineering, pp. 81-89.

[10] Berdichevsky, V., Armanios, E.A. , and Badir, A.,1992. "Theory of Anisotropic Thin Walled Closed Cross Section Beams," Composites Engineering, Vol. 2, No. 5-7, pp. 411-432.

[11] Bauchau, O. A., and Hodges, D.H., 1999. "Analysis of Nonlinear Multi-Body Systems with Elastic Couplings," Multibody System Dynamics, Vol 3, pp. 168-188.

[12] Chandra, R. and Chopra, I., 1992. "Structural Response of Composite Beams and Blades with Elastic Couplings," Composites Engineering, Vol. 2 (5-7), pp. 347-374.

[13] Armanios, E. A., Makeev, A., Hooke, D. A., 1996. "Finite Displacement Analysis of Laminated Composite Strips with Extension-Twist Coupling", Journal of Aerospace Engineering, Vol. 9, No. 3, July, pp. 80-91.

[14] Armanios, E. A., Hooke, D., Kamat, M., Palmer, D., and Li, J., 1993. "Design and Testing of Composite Laminates with Optimum Extension-twist Coupling," Camponeschi Jr., E. T. (Ed), Composite Materials: Testing and Design, Vol. 11, ASTM STP 1206, American Society for Testing and Materials, Philadelphia, PA, pp. 249-262.

[15] Ozbay, S., 2006. "Extension-twist Coupling in Composite Rotor blades," PhD Thesis, School of Aerospace Engineering, Georgia Institute of Technology.

[16] Cross, R.J., Haynes, R.A., and Armanios, E.A., 2007. "Design of Hygrothermally Stable Laminated Composites for Extension-Twist Coupling," Proceedings of American Society for Composites, 22nd Annual Technical Conference, Seattle, WA, September.

[17] Badir, A. M., "Theory of Anisotropic Thin-Walled Closed-Section beams with Hygrothermal Effects," *33rd AIAA/ASME/ASCE/AHS/ASC structures, Structural Dynamics and Materials (SDM)Conference,* Dallas, TX, AIAA-92-2543-CP, pp. 1078-1092

[18] Yu, W., 2001. “VABS Manual for Users,” pp. 1-3.

BIOGRAPHICAL INFORMATION

Sean Christopher Muder was born in Overland Park, Kansas on March 20, 1988. He graduated from Lawrence High School in May, 2006. He attended Austin College in Sherman Texas and obtained a Bachelor of Arts in Physics. He enrolled in the master's degree program at the University of Texas Arlington in August 2010 and has plans of continuing his education to obtain a Ph.D in Aerospace Engineering.

In addition to his studies, Sean was a four year varsity letterman in baseball at Austin College. He was honored his senior year with the Slats McCord award for being the most dedicated male senior athlete.